Plasma flow in peripheral region of detached plasma in linear plasma device

Cite as: Phys. Plasmas **23**, 012511 (2016); https://doi.org/10.1063/1.4940310
Submitted: 09 July 2015 • Accepted: 04 January 2016 • Published Online: 21 January 2016

Y. Hayashi, N. Ohno, S. Kajita, et al.

Plasma flow in peripheral region of detached plasma in linear plasma device

Y. Hayashi,[1,a)] N. Ohno,[1] S. Kajita,[2] and H. Tanaka[3]
[1]*Graduate School of Engineering, Nagoya University, Nagoya, Aichi 464-8603, Japan*
[2]*EcoTopia Science Institute, Nagoya University, Nagoya, Aichi 464-8603, Japan*
[3]*National Institute for Fusion Science, Toki, Gifu 509-5292, Japan*

(Received 9 July 2015; accepted 4 January 2016; published online 21 January 2016)

A plasma flow structure is investigated using a Mach probe under detached plasma condition in a linear plasma device NAGDIS-II. A reverse flow along the magnetic field is observed in a steady-state at far-peripheral region of the plasma column in the upstream side from the recombination front. These experimental results indicate that plasma near the recombination front should strongly diffuse across the magnetic field, and it should be transported along the magnetic field in the reverse flow direction. Furthermore, bursty plasma density fluctuations associated with intermittent convective plasma transport are observed in the far-peripheral region of the plasma column in both upstream and downstream sides from the recombination front. Such a nondiffusive transport can contribute to the intermittent reverse plasma flow, and the experimental results indicate that intermittent transports are frequently produced near the recombination front. © *2016 AIP Publishing LLC*.
[http://dx.doi.org/10.1063/1.4940310]

I. INTRODUCTION

It is important to study the structure of plasma flow along magnetic field lines in the scrape-off layer (SOL) of magnetically confined fusion devices.[1] Plasma flow influences the impurity transport, impurity screening properties, and profile of material deposition on plasma facing components (PFCs). In addition, the SOL current, which is an important flow in the SOL, causes the asymmetry of inner-and-outer divertor plasma.[2] This asymmetry affects the formation of detached plasma and particle control with pumping in the divertor region. Many SOL flow measurements by using Mach probes were performed at different poloidal locations in tokamak devices such as JT-60U,[3,4] JET,[5,6] AlcatorC-Mod,[7,8] TCV,[9] DIII-D,[10] ASDEX-Upgrade,[11,12] and ToreSupra.[13] It is suggested that the stagnation point is between the low field side (LFS) midplane and the LFS SOL near the X-point. Furthermore, a subsonic flow with a parallel Mach number of 0.2–1.0 was observed from the LFS SOL to the high field side (HFS) divertor in the lower single null (LSN) divertor geometry. This flow pattern was described for several reasons, e.g., the ion $\boldsymbol{B} \times \nabla B$ drift toward the divertor, plasma pressure difference between the HFS and the LFS SOL,[14] and asymmetry of the inner-and-outer divertor plasma.

On the other hand, a detached divertor operation is proposed because it has the potential to reduce the high heat and particle fluxes in the divertor plate.[15] For detaching the plasma from the divertor plate, it is necessary to increase the neutral gas pressure by applying additional gas puffing or by enhancing particle recycling. Some experiments on the static and dynamic plasma behaviors at a high neutral pressure were conducted using linear plasma devices NAGDIS-II,[16,17] MAP-II,[18] and PISCES-A.[19] In addition, plasma flow was also measured by varying the neutral gas pressure, P, in a range of 2–35 mTorr in NAGDIS-II.[20] The flow reversal in the axial direction was observed in the edge region when the neutral pressure was high (35 mTorr). The mechanism of reverse plasma flow is not fully understood yet.

In this study, in order to understand the reverse plasma flow mechanism, we measured plasma flow in the axial direction by using a Mach probe in the detached plasma of NAGDIS-II. The experiment was conducted by focusing on the position of the recombination front in the detached plasma, and some statistical data processing techniques were used to analyze the experimental data.

II. EXPERIMENTAL SETUP

Fig. 1 shows a schematic view of the Mach probe head used for this study. Two tungsten electrodes were placed 0.8 mm inside an alumina tube. The dimension of the exposed area of each electrode was 0.8 mm in diameter. The bias voltage for both electrodes was −200 V in order to measure the ion saturation current (I_{sat}) during the experiment.

The experiments were performed using NAGDIS-II.[21] The device generated high-density helium plasma with an electron density of up to $10^{20}\,m^{-3}$ in a steady-state. The magnetic field strength was 0.2 T in this experiment. The device had a plasma discharge region and a divertor test region, where the diameter of the plasma column was approximately 20 mm. The length of the plasma column was approximately 2 m, and it was terminated with a floating target plate. When the neutral gas pressure was increased in the divertor test region, the detached plasma was formed, while the parameters in the plasma source region were almost constant because the configuration of the device could create a pressure difference of two orders magnitude between the divertor test region and the plasma discharge region. Under the detached plasma condition, both ionizing and recombining plasma coexisted along the magnetic field. The ionizing plasma and the recombining plasma were located in

a)Author to whom correspondence should be addressed. Electronic mail: hayashi-yuki13@ees.nagoya-u.ac.jp

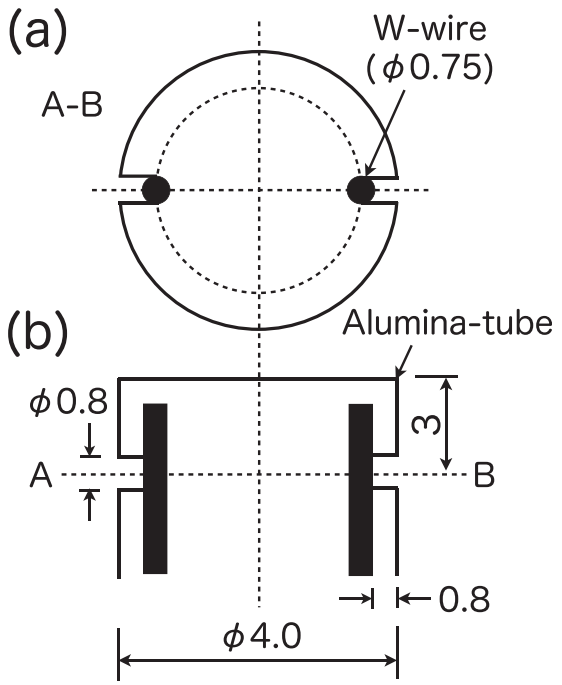

FIG. 1. (a) Schematics of the Mach probe head designed for plasma flow measurement. (a) The cross section in A and B planes; (b) the side view of the structure.

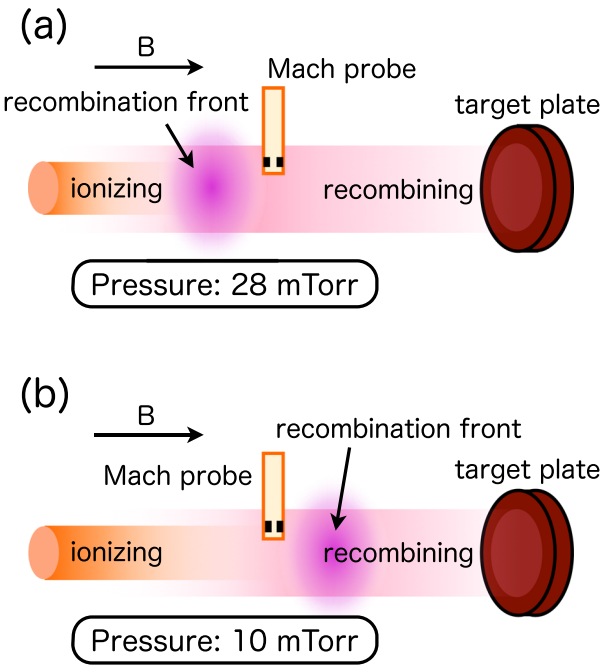

FIG. 2. Schematics representing the position of the Mach probe against the recombination front under the conditions of (a) a high neutral pressure ($P \sim 28$ mTorr) and (b) a low neutral pressure ($P \sim 10$ mTorr).

upstream and downstream sides, respectively. The recombination front, which was located between the ionizing and recombining plasma, played an important role in the plasma detachment. At the recombination front, where the strong emissions from highly excited levels were observed, low-temperature and high-density plasma was disappeared due to the volumetric recombination.[22–24] The axial position of the recombination fronts was shifted by controlling the neutral gas pressure.

The Mach probe was set along the magnetic field to measure plasma flow along the magnetic field. Plasma flow was measured under conditions that the Mach probe was downstream (Fig. 2(a)) and upstream (Fig. 2(b)) from the recombination front. The pressure, which was measured near the Mach probe, was 28 and 10 mTorr in the former and latter cases, respectively. Fig. 3 shows the radial profile of the time-averaged I_{sat} in NAGDIS-II measured using a single Langmuir probe at the same axial position as the Mach probe at P of 28 and 10 mTorr. As shown in Fig. 3, in this study, the flow measurement was conducted in the peripheral region of the plasma column.

III. EXPERIMENTAL RESULTS AND ANALYSIS

A. Measurement of the ion saturation current

Figs. 4(a) and 5(a) show the time evolution of I_{sat} measured by two electrodes (facing the upstream and downstream sides) of the Mach probe at a radial position, r, of 30 mm when the Mach probe is downstream and upstream from the recombination front, respectively. In addition, Figs. 4(b) and 5(b) show the Mach number M_i evaluated by the following relation[25,26] by using the measured I_{sat}

$$M_i = M_c \ln \frac{I_{up}}{I_{down}}, \quad (1)$$

where I_{up} and I_{down} are the measured I_{sat} of the upstream and downstream probes, respectively. When I_{up} is greater than I_{down}, plasma flows toward the target plate, and the sign of M_i is denoted by plus. M_c is assumed 0.45, which is a typical value under the condition of an approximate equality of the ion and electron temperatures.[27] Further accurate estimation of the plasma flow velocity requires valid models. In this study, the relative values of the Mach number are mainly discussed.

We show typical examples of the temporal evolution of I_{sat} and the Mach number in Figs. 4 and 5. When the Mach probe is located downstream from the recombination front,

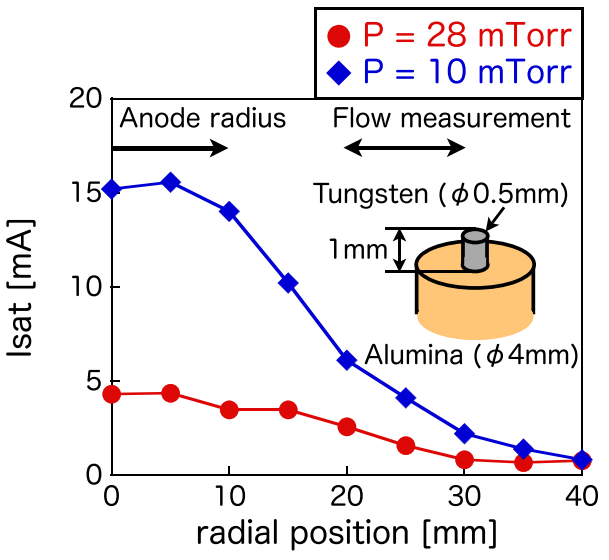

FIG. 3. Radial profile of I_{sat} measured using a single Langmuir probe at a neutral pressure of 28 mTorr and 10 mTorr.

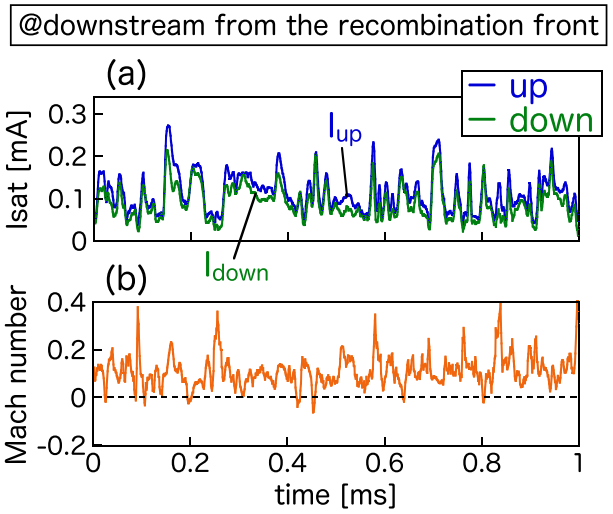

FIG. 4. Typical time evolutions of (a) I_{sat} measured by each probe and (b) the Mach number when the Mach probe is downstream from the recombination front at $P \sim 28$ mTorr.

I_{up} is greater than I_{down}. Moreover, Fig. 4(b) shows that the Mach number is positive for a long time. These results indicate that mean plasma flow is from the plasma source region toward the target. In contrast, when the Mach probe is upstream from the recombination front, I_{down} is greater than I_{up}. Hence, the Mach number shown in Fig. 5(b) is negative. This indicates that plasma flow reversal occurred by changing the relative position of the Mach probe to the recombination front.

B. Probability density function (PDF) and the radial profile of the Mach number

Figs. 6(a) and 6(b) show the PDF of the Mach number, comparing three different radial positions in the peripheral region of the plasma column. When the Mach probe is downstream from the recombination front (Fig. 6(a)), the PDF has a peak near $M_i \sim 0.1$ for all radial positions. This indicates that plasma flow from the plasma source region to the target plate is dominant. However, in Fig. 6(b), the PDF profiles

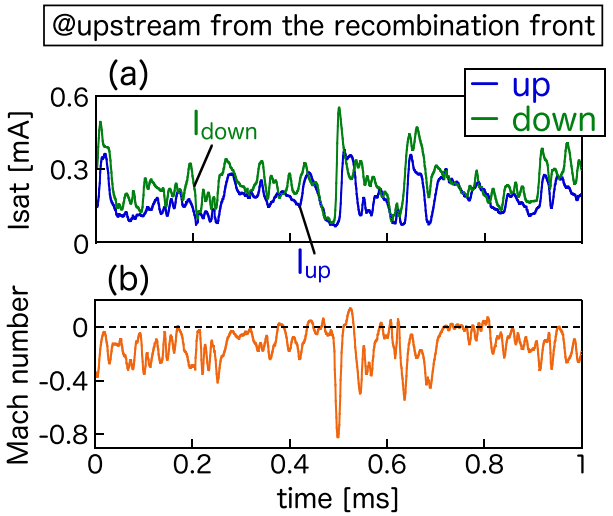

FIG. 5. Typical time evolutions of (a) I_{sat} measured by each probe and (b) the Mach number when the Mach probe is upstream from the recombination front at $P \sim 10$ mTorr.

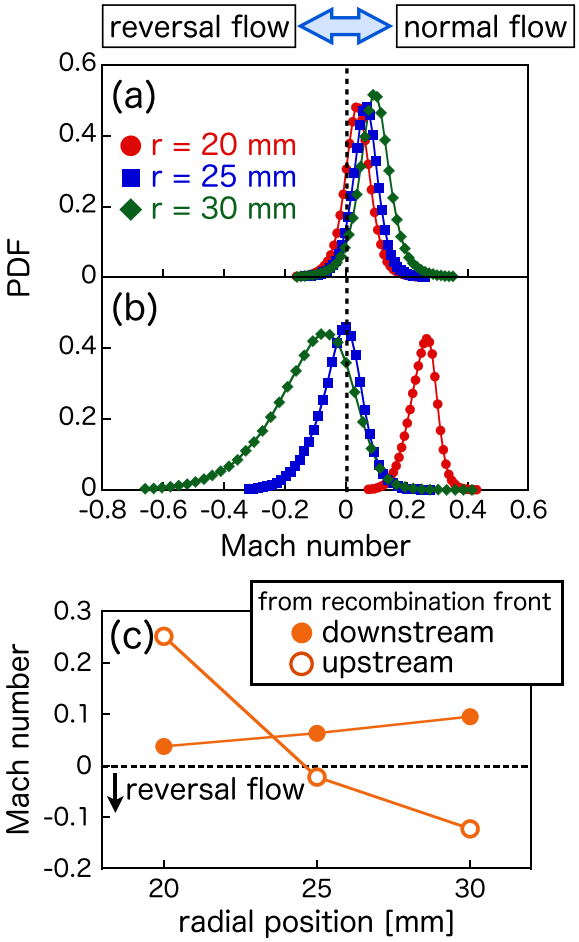

FIG. 6. Probability density functions (PDFs) of the Mach number at $r = 20$, 25, and 30 mm, respectively, in cases if the Mach probe is (a) downstream and (b) upstream from the recombination front. (c) The radial profile of the time-averaged Mach number when the Mach probe is downstream (closed circles) and upstream (open circles) from the recombination front.

shift toward the negative side especially at $r = 30$ mm, while the PDF profile at $r = 20$ mm is in more positive side rather than Fig. 6(a). This means that plasma flows toward the target plate inside and near the plasma column in the upstream region, and flow reversal occurs in the far-peripheral region of the plasma column. Fig. 6(c) shows the radial profile of the time-averaged Mach numbers in the upstream and downstream sides. In the downstream side, the Mach number is positive in all radial positions and gradually increases with r. At $r = 20$ mm, the Mach number in the upstream side ($M_i \sim 0.25$) is greater than that in the downstream side. This demonstrates that the main plasma flow inside the plasma column in the upstream region decreases along the magnetic field induced by momentum losses due to the volumetric recombination and charge exchange processes near the recombination front.

C. Skewness of the ion saturation current and the Mach number

Skewness is defined by the third moment of the PDF as $S = \langle \tilde{I}_{sat}^3 \rangle / \langle \tilde{I}_{sat}^2 \rangle^{3/2}$, and it describes the asymmetry property of the PDF profile. If random processes are dominant, the PDF profile follows the Gaussian distribution and $S = 0$. In

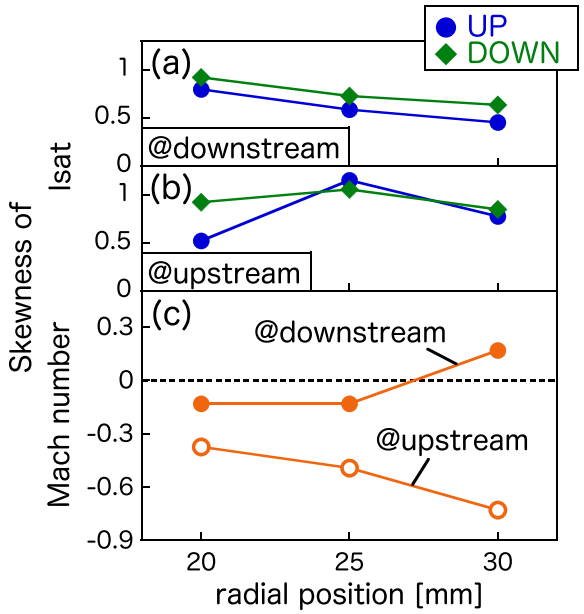

FIG. 7. Radial profiles of the skewness of I_{sat} (I_{up} and I_{down}) when the Mach probe is (a) downstream and (b) upstream from the recombination front, respectively, and (c) the skewness of the Mach number when the Mach probe is downstream (closed circles) and upstream (open circles) from the recombination front.

particular, in a situation, in which bursty transport occurs frequently, the waveform of I_{sat} has a number of positive spikes, and consequently, $S > 0$. The skewness of I_{sat} from each probe is shown in Figs. 7(a) and 7(b). It is consistently positive at all radial positions when the Mach probe is downstream (Fig. 7(a)) and upstream (Fig. 7(b)) from the recombination front. This means that the waveforms of I_{sat} include several positive spikes and bursty transport occurs frequently. Moreover, Fig. 7(c) indicates that the skewness of the Mach number is negatively larger upstream from the recombination front (open circles) than downstream (closed circles). Because the sign of the Mach number in the far-peripheral region (especially at $r = 30$ mm) is also negative (Fig. 6(c)), the intermittent reverse flow toward the plasma source region can be generated outside the plasma column. Although the Mach probe theory can be applied to evaluate the mean flow in a steady-state condition, the time lag of I_{sat} spikes shows the existence of such intermittent transports towards the plasma source region and is described in Sec. IV.

IV. DISCUSSION

Fig. 8 shows a schematic view of the plasma flow structure as the summary of experimental results described in Section III, typical photographs showing the transition from ionizing plasma to recombining plasma taken from the observation windows, and profiles of the electron temperature, T_e, and the electron density, n_e, under the detached condition along the magnetic field. The arrow size denotes the steady flow amplitude, based on the Mach number profile demonstrated in Fig. 6(c). As mentioned above, plasma flow reversal exists in the far-peripheral region of the upstream side.

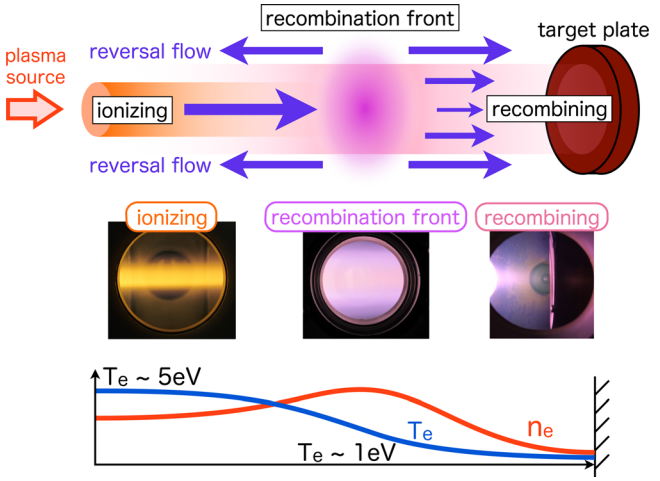

FIG. 8. Schematics representing plasma flow structure, typical photographs showing the transition from attached to detached plasma taken from the observation windows, and axial profiles of the electron temperature, and electron density under the detached condition in NAGDIS-II.

Because the electron impact ionization process produces high-density plasma near the recombination front, plasma can strongly diffuse across the magnetic field due to the radial density gradient. The photograph also shows a wide plasma distribution near the recombination front. Then, plasma diffused to the far-peripheral region is transported along the magnetic field in both directions to the plasma source region (upstream) and to the target plate (downstream). Hence, the axial localization of an increased density near the recombination front should lead to an axially localized increased radial transport to the periphery, which then drains along the magnetic field away from the recombination front owing to parallel transport, leading to the observed flow pattern. One of the reasons for generating the axially localized enhancement of radial transport should be the enhanced diffusion process across the magnetic field near the recombination front. For quantifying the radial particle transport, the direct measurements by using the electrostatic probes, which can estimate the radial flux across the magnetic field, are part of the future work.

A second possible reason is the intermittent cross-field transport observed in linear magnetized plasma.[28–31] It attracted attention as the similar transport associated with plasma blobs observed in other magnetically confined fusion devices.[32–34] Plasma blob is a large-scale structure of plasma with a large radial velocity, and it is transported convectively owing to the effect of the curvature and gradient of the magnetic field in the fusion devices. As assumed, because there is neither curvature nor gradient of the magnetic field in linear plasma devices, intermittent transport is driven by the centrifugal force of plasma rotation or the effect of a neutral wind, which is generated by a charge exchange process in the plasma column.[35] These intermittent plasma transports, having a higher density than the ambient plasma in the peripheral region, are extended along the magnetic field lines after detaching from the bulk plasma and then form filamentary structures. Reference 28 reported the detailed analytical results on 2D motion across the magnetic field of coherent

structures under the detached plasma condition in NAGDIS-II. Movies taken by a fast-imaging camera show the dynamics of a 2D spiral structure in the peripheral regions ($r \sim 25$ mm) of the plasma column. This spiral structure is radially localized and propagated far from the plasma column. Because the skewness of I_{sat} is a large positive value in this experiment, many positive spikes appear in I_{sat}. The result indicates that bursty plasma transport occurs frequently in the peripheral region.

Fig. 9 shows the time evolution of the I_{sat} measured in the so-far-peripheral region ($y = 60$ mm) at different neutral pressures.[36] When the neutral pressure is increased to produce the fully detached plasma, positive spikes in I_{sat} become wider and their amplitudes increase. Further, although the averaged I_{sat} at the center of the plasma column dramatically decreases the averaged value of I_{sat} increases with the neutral pressure, as shown in Fig. 9. It is demonstrated that the intermittent plasma transport is enhanced under the detached condition and the cross-field transport, depositing the density in the periphery, should lead to broadening the plasma profile. This large plasma profile achieved by the intermittent plasma transport plays an important role in the reduction of the particle and heat flux in the divertor plate.[28,37] In addition to the recombining processes in the detached plasma, broadening of the plasma profile reduces the local loads to the divertor and prolongs the lifetime of the PFCs.

The radial intermittent cross-field plasma transport observed in the linear plasma device was reproduced in kinetic numerical simulation.[38] It was shown that 3D simulations based on a well-established model of drift-fluid dynamics reproduced many features of a spiraling intermittent motion in NAGDIS-II. A broad qualitative agreement is found with respect to statistical properties and coherent structures. It was concluded that the plasma source is axially localized along the magnetic field, and it produces plasma instability, which generates filamentary plasma structures in the peripheral region of the plasma column. The localized plasma source in the simulation is likely to correspond to the recombination front in the detached plasma. In order to reveal the behavior of plasma instability under the detached condition, further experiments and theoretical studies are needed.

In order to obtain typical waveforms of I_{sat} spike, a conditional averaging method is employed. Fig. 10(a) shows the conditional averaged I_{up} and I_{down} when reverse plasma flow occurs at $r = 30$ mm and the Mach probe is upstream from the recombination front. In this analysis, large bursts of I_{down} with a larger peak than $2\sigma + \mu$ of the original waveform are selected and averaged in the same time domain, where σ and μ are the standard deviation and the averaged value, respectively. I_{up} is obtained from the original waveform in the time range corresponding to the time window for selecting I_{down}. The result shows that the positive spike exhibits a rapid increase and a slow decay. This actually resembles the averaged shape of I_{sat} measured in Large Helical Device (LHD) and JT-60U.[37,39] These results support the fact that the intermittent convective transports are frequently generated at the recombination front.

A time delay of 5 μs between the I_{down} peak and the I_{up} peak was observed. The cross correlation coefficient[39,40] between the I_{up} and the I_{down} is given by

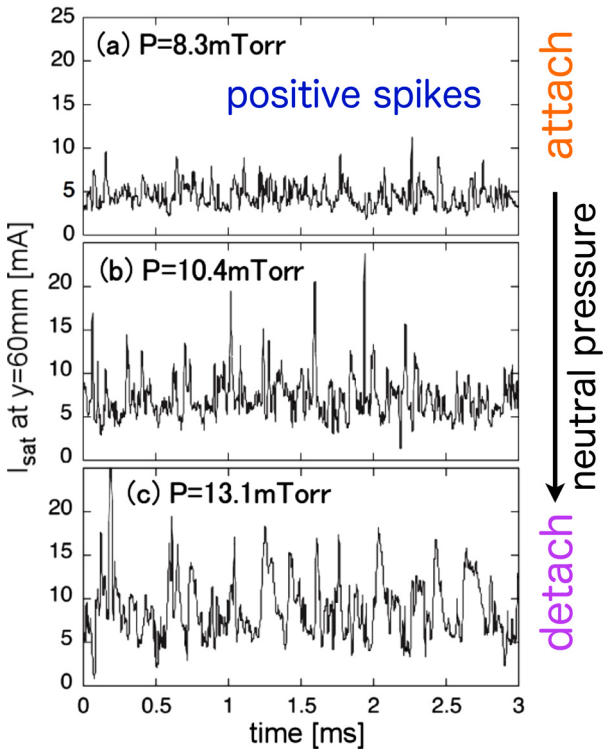

FIG. 9. Neutral pressure dependence of the I_{sat} waveforms in the peripheral region of NAGDIS-II. Reprinted with permission from Ohno *et al.*, J. Plasma Fusion Res. **80**, 275 (2004). Copyright 2009 The Japan Society of Plasma Science and Nuclear Fusion Research.

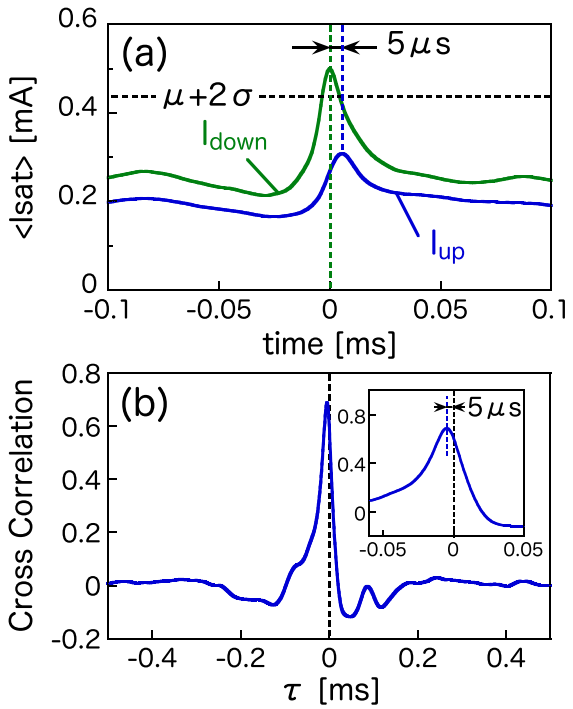

FIG. 10. (a) Conditional averaged I_{up} and I_{down} at $r = 30$ mm when the Mach probe is upstream from the recombination front and (b) the cross correlation coefficient between I_{up} and I_{down}. σ and μ are the standard deviation and averaged value, respectively.

$$R_{I_{\rm up}I_{\rm down}}(\tau) = \frac{\langle \tilde{I}_{\rm up}(t)\tilde{I}_{\rm down}(t+\tau)\rangle}{\langle \tilde{I}^2_{\rm up}\rangle^{1/2}\langle \tilde{I}^2_{\rm down}\rangle^{1/2}}, \quad (2)$$

and also shown in Fig. 10(b). Here, $\langle\rangle$ indicates the averaging, $\tilde{I}$ denotes the fluctuation component, $(I-\langle I\rangle)$, and τ is the time delay. In this analysis, all waveforms of $I_{\rm sat}$ are calculated for correlation. The correlation peak is located at $\tau = -5\,\mu$s ($I_{\rm up}$ has a delay), and the time delay of 5 μs is the same as for conditional averaging. Therefore, even from the correlation analysis, intermittent transport is dominant at $r = 30$ mm upstream from the recombination front. As the diameter of the Mach probe is 4 mm, the velocity of intermittent transport across the Mach probe is estimated as ~800 m/s. On the other hand, the edge plasma should be typically transported at 0.2 times the ion sound speed. The ion sound speed $C_s = \sqrt{e(T_e[\mathrm{eV}] + T_i[\mathrm{eV}])/m_i}$ [m/s] in the peripheral region could be estimated by using the $T_{\rm e}$ measured using a spectroscopic method, where e is the elementary electric charge and $m_{\rm i}$ is the helium ion mass. In order to determine $T_{\rm e}$ by using spectroscopy, it was decided to perform a Boltzmann plot of a series of Balmer-type lines, which are the transitions from highly excited levels to $n = 2$ level, for helium atoms, where n is the principal quantum number.[41,42] In this experiment, $T_{\rm e} \sim 0.13$ eV obtained using spectroscopy leads to $0.2C_{\rm s} \sim 500$ m/s, which indicates that the velocity of intermittent transport is greater than that of the steady-state plasma flow along the magnetic field.

For future fusion devices, the reverse transport toward the core plasma from the recombination front will be an issue because the impurity particles and low temperature plasma produced by plasma-material and plasma-gas interactions in the divertor region degrade the core plasma confinement. Moreover, intermittent plasma flow, which is generated at the recombination front and transported with a higher velocity than the steady flow, affects the impurity transport owing to the friction force. In Ref. 1, the edge flow measurements performed for L-mode plasma at various poloidal positions in tokamak devices with the divertor configuration are reported. It was discussed that the stagnation point should be between the LFS midplane and the LFS SOL near the X-point in future experimental devices such as ITER. Reverse flow from the divertor region contributes to the shift of the stagnation point towards the LFS midplane. Furthermore, the impurity particles might not reach the divertor because they can be stopped and accumulated in the front of the recombination front, which is an effective plasma source under the detached plasma condition.

V. CONCLUSION

In order to understand the reverse plasma flow mechanism, the flow structure was investigated using a conventional Mach probe under the detached plasma condition in linear plasma device NAGDIS-II. The time evolution of the ion saturation current shows the existence of steady-state reverse flow in the upstream side from the recombination front. In addition, the PDF shows that reverse flow occurs in the far-peripheral region of the plasma column. These results can be described with the diffusion process across the magnetic field caused by the radial density gradient near the recombination front. Furthermore, the bursty plasma transport was observed by calculating the skewness of the $I_{\rm sat}$. The intermittent cross-field transport should be one of the causes for enhancing the radial transport to the periphery, which then drains along the magnetic field away from the recombination front owing to parallel transport. The velocity of intermittent transport across the Mach probe calculated from the time lag of the $I_{\rm sat}$ spikes in the conditional averaging waveforms is greater than that of steady-state plasma flow estimated by an optical method.

ACKNOWLEDGMENTS

This work was supported by JSPS KAKENHI Grant Number (25289337). This work is partially supported by NIFS/NINS under the project of Formation of International Network for Scientific Collaborations and NIFS Collaboration Research Program (NIFS14KUGM094).

[1]N. Asakura, and ITPA SOL and Divertor Topical Group, J. Nucl. Mater. **363–365**, 41 (2007).
[2]N. Hayashi, T. Takizuka, A. Hatayama, and M. Ogasawara, Nucl. Fusion **38**, 1695 (1998).
[3]N. Asakura, S. Sakurai, N. Hosogane, M. Shimada, K. Itami, Y. Koide, and O. Naito, Nucl. Fusion **39**, 1983 (1999).
[4]N. Asakura, H. Takenaga, S. Sakurai, H. Tamai, A. Sakasai, K. Shimizu, and G. D. Porter, Plasma Phys. Controlled Fusion **44**, 2101 (2002).
[5]S. K. Erents, A. V. Chankin, G. F. Matthews, and P. C. Stangeby, Plasma Phys. Controlled Fusion **42**, 905 (2000).
[6]S. K. Erents, R. A. Pitts, W. Fundamenski, J. P. Gunn, and G. F. Matthews, Plasma Phys. Controlled Fusion **46**, 1757 (2004).
[7]B. LaBombard, J. A. Goetz, I. H. Hutchinson, D. Jablonski, J. Kesner, C. Kurz, B. Lipschultz, G. M. McCracken, A. Niemczewski, J. Terry, A. Allen, R. L. Boivin, F. Bombarda, P. Bonoli, C. Christensen, C. Fiore, D. Gamier, S. Golovato, R. Granetz, M. Greenwald, S. Home, A. Hubbard, J. Irby, D. Lo, D. Lumma, E. Marmar, M. May, A. Mazurenko, R. Nachtrieb, H. Ohkawa, P. O'Shea, M. Porkolab, J. Reardon, J. Rice, J. Rost, J. Schachter, J. Snipes, J. Sorci, P. Stek, Y. Takase, Y. Wang, R. Watterson, J. Weaver, B. Welch, and S. Wolfe, J. Nucl. Mater. **241–243**, 149 (1997).
[8]B. LaBombard, J. E. Rice, A. E. Hubbard, J. W. Hughes, M. Greenwald, R. S. Granetz, J. H. Irby, Y. Lin, B. Lipschultz, E. S. Marmar, K. Marr, D. Mossessian, R. Parker, W. Rowan, N. Smick, J. A. Snipes, J. L. Terry, S. M. Wolfe, S. J. Wukitch, and the Alcator C-Mod Team, Nucl. Fusion **44**, 1047 (2004).
[9]R. Pitts, J. Horacek, W. Fundamenski, O. E. Garcia, A. H. Nielse, M. Wischmeier, V. Naulin, and J. J. Rasmussen, J. Nucl. Mater. **363–365**, 505 (2007).
[10]J. A. Boedo, R. Lehmer, R. A. Moyer, J. A. Boedo, R. Lehmer, R. A. Moyer, J. G. Watkins, G. D. Porter, T. E. Evans, A. W. Leonard, and M. J. Schaffer, J. Nucl. Mater. **266–269**, 783 (1999).
[11]M. Tsalas, D. Coster, C. Fuchs, A. Herrmann, A. Kallenbach, H. W. Mueller, J. Neuhauser, V. Rohde, N. Tsois, and The ASDEX Upgrade Team, J. Nucl. Mater. **363–365**, 1093 (2007).
[12]H. W. Müller, V. Bobkov, A. Herrmann, M. Maraschek, J. Neuhauser, V. Rohde, A. Schmid, M. Tsalas, and ASDEX Upgrade Team, J. Nucl. Mater. **363–365**, 605 (2007).
[13]J. P. Gunn, C. Boucher, M. Dionne, I. Ďuran, V. Fuchs, T. Loarer, I. Nanobashvili, R. Pánek, J.-Y. Pascal, F. Saint-Laurent, J. Stöckel, T. Van Rompuy, R. Zagórski, J. Adámek, J. Bucalossi, R. Dejarnac, P. Devynck, P. Hertout, M. Hron, G. Lebrun, P. Moreau, F. Rimini, A. Sarkissian, and G. Van Oost, J. Nucl. Mater. **363–365**, 484 (2007).
[14]B. LaBombard, J. E. Rice, A. E. Hubbard, J. W. Hughes, M. Greenwald, R. S. Granetz, J. H. Irby, Y. Lin, B. Lipschultz, E. S. Marmar, K. Marr, D. Mossessian, R. Parker, W. Rowan, N. Smick, J. A. Snipes, J. L. Terry, S. M. Wolfe, S. J. Wukitch, and the Alcator C-Mod Team, Phys. Plasmas **12**, 056111 (2005).

[15]ITER Physics Expert Group on Divertor, ITER Physics Expert Group on Divertor Modelling and Database, and ITER Physics Basis Editors, Nucl. Fusion **39**, 2391 (1999).
[16]N. Ezumi, S. Mori, N. Ohno, M. Takagi, S. Takamura, H. Suzuki, and J. Park, J. Nucl. Mater. **241–243**, 349 (1997).
[17]N. Ezumi, N. Ohno, K. Aoki, D. Nishijima, and S. Takamura, Contrib. Plasma Phys. **38**, 31 (1998).
[18]A. Okamoto, S. Kado, Y. Iida, and S. Tanaka, Contrib. Plasma Phys. **46**, 416 (2006).
[19]E. M. Hollmann, C. Brandt, B. Hudson, D. Kumar, D. Nishijima, and A. Yu. Pigarov, Phys. Plasmas **20**, 093303 (2013).
[20]E.-K. Park, H.-J. Woo, K.-S. Chung, H. Tanaka, S. Kajita, and N. Ohno, Curr. Appl. Phys. **12**, 1497 (2012).
[21]N. Ohno, D. Nishijima, S. Takamura, Y. Uesugi, M. Motoyama, N. Hattori, H. Arakawa, N. Ezumi, S. Krasheninnikov, A. Pigarov, and U. Wenzel, Nucl. Fusion **41**, 1055 (2001).
[22]F. Scotti, S. Kado, A. Okamoto, T. Shikawa, Y. Kuwahara, K. Kurihara, K. Chung, and S. Tanaka, Plasma Fusion Res. **2**, S1110 (2007).
[23]F. Scotti and S. Kado, J. Nucl. Mater. **390–391**, 303 (2009).
[24]S. Kado, J. Nucl. Mater. **463**, 902 (2015).
[25]K.-S. Chung and I. H. Hutchinson, Phys. Rev. A **38**, 4721 (1988).
[26]K.-S. Chung and I. H. Hutchinson, Phys. Fluids B **3**, 3053 (1991).
[27]I. H. Hutchinson, Plasma Phys. Controlled Fusion **44**, 1953 (2002).
[28]H. Tanaka, N. Ohno, Y. Tsuji, and S. Kajita, Contrib. Plasma Phys. **50**, 256 (2010).
[29]H. Tanaka, N. Ohno, Y. Tsuji, K. Okazaki, and S. Kajita, Contrib. Plasma Phys. **52**, 424 (2012).
[30]G. Y. Antar, S. I. Krasheninnikov, P. Devynck, R. P. Doerner, E. M. Hollmann, J. A. Boedo, S. C. Luckhardt, and R. W. Conn, Phys. Rev. Lett. **87**, 065001 (2001).
[31]T. A. Carter, Phys. Plasmas **13**, 010701 (2006).
[32]G. Y. Antar, G. Counsell, Y. Yu, and P. Devynck, Phys. Plasmas **10**, 419 (2003).
[33]S. I. Krasheninnikov, Phys. Lett. A **283**, 368 (2001).
[34]O. Grulke, J. L. Terry, B. LaBombard, and S. J. Zweben, Phys. Plasmas **13**, 012306 (2006).
[35]S. I. Krasheninnikov and A. I. Smolyakov, Phys. Plasmas **10**, 3020 (2003).
[36]N. Ohno, K. Furuta, and S. Takamura, J. Plasma Fusion Res. **80**, 275 (2004).
[37]H. Tanaka, N. Ohno, Y. Tsuji, S. Kajita, S. Masuzaki, M. Kobayashi, T. Morisaki, H. Tsuchiya, A. Komori, and the LHD Experimental Group, Phys. Plasmas **17**, 102509 (2010).
[38]D. Reiser, N. Ohno, H. Tanaka, and L. Vela, Phys. Plasmas **21**, 032302 (2014).
[39]H. Tanaka, N. Ohno, N. Asakura, Y. Tsuji, H. Kawashima, S. Takamura, Y. Uesugi, and the JT-60 Team, Nucl. Fusion **49**, 065017 (2009).
[40]P. F. Dunn, *Measurement and Data Analysis for Engineering and Science*, 2nd ed. (Taylor & Francis/CRC Press, Boca Raton, 2010).
[41]D. Nishijima, U. Wenzel, K. Ohsumi, N. Ohno, Y. Uesugi, and S. Takamura, Plasma Phys. Controlled Fusion **44**, 597 (2002).
[42]N. Ohno, M. Tanaka, N. Ezumi, D. Nishijima, S. Takamura, S. I. Krasheninnikov, A. Yu. Pigarov, and J. Park, Phys. Plasmas **6**, 2486 (1999).